JOURNAL OF AGRICULTURAL AND FOOD CHEMISTRY
ARTICLE

J. Agric. Food Chem. 2010, 58, 1275–1282 1275
DOI:10.1021/jf9032393

Starch Molecular Structure Shows Little Association with Fruit Physiology and Starch Metabolism in Tomato

Kietsuda Luengwilai,[†] Kanitha Tananuwong,[§] Charles F. Shoemaker,[‡] and Diane M. Beckles*,[†]

[†]Department of Plant Sciences MS-3, and [‡]Department of Food Sciences, University of California, One Shields Avenue, Davis, California 95616, and [§]Department of Food Technology, Faculty of Science, Chulalongkorn University, Bangkok 10330, Thailand

The aim of this work was to determine if the molecular structure of starch from tomato (*Solanum lycopersicum* L.) is influenced by fruit physiology and carbohydrate metabolism. The effect of fruit size, fruit ripening behavior, and assimilate availability on starch granule accumulation was examined in nine tomato samples. The percentage of ^{14}C-glucose partitioning to starch was similar among samples, but starch contents varied 10-fold, suggesting differences in metabolism. In contrast, granule size (10−20 μm), amylose content (19−23%), degree of crystallinity (26-31%), and enthalpy of gelatinization (14.8−17.2 °C) were similar. Some differences in structure were detected in starch from the largest and smallest fruit using more sensitive analyses such as thermal properties, chain length distribution of amylopectin, and susceptibility to *in vitro* α-amylase digestion. However, overall, our results suggest that granule characteristics are highly conserved in tomato fruit, and we conclude that this is likely due to inherent metabolic constraints.

KEYWORDS: Tomato; starch structure; starch properties; starch biosynthesis

INTRODUCTION

Starch biosynthesis in tomato (*Solanum lycopersicum* L.) is important from a food and agricultural perspective. Starch granules may give green tomato fruit key textural and physicochemical properties that make them suitable for foods such as chutneys, relishes, and green fried tomatoes. From an agricultural standpoint, starch may be an important determinant of tomato crop yield. Its accumulation in the earliest stages of fruit development may help to increase import of photosynthate leading to higher dry matter content (*1*−*3*). Furthermore, in several cultivars, starch degraded to sugars during ripening makes a significant contribution to fruit soluble solids and hence to quality (*3*,*4*). Still, in spite of the importance of tomato as a horticultural crop (world production is ∼1.26 million metric tonnes pa) and the potential role starch metabolism plays in determining fruit yield and quality, comparatively little is known about starch granule characteristics in this species.

Aside from economic considerations, tomato starch may also be important as a model to study starch-metabolism−molecular-structure relationships. (i) Manipulating fruit sugar supply, physiology, and metabolism can be easily done by pruning, that is, changing the plant leaf-to-fruit ratio, and the effect on starch monitored (*5*, *13*). (ii) Examining tomato starch may offer novel insight on starch biosynthesis. Tomato may be considered to make "transitory-storage" starch. This starch is synthesized over longer periods than that for leaf "transitory" starches but much shorter than that for the "storage" starches of heterotrophic tissues before degradation, and this could influence granule characteristics. (iii) Finally, in contrast to most plants studied, starch accumulation in tomato fruit may be subject to turnover, that is, simultaneous synthesis and degradation (*1*), and differ from the temporally separated cycles of synthesis and degradation in other tissues; how or if this influences granule properties is unknown.

The aim of this work was to determine the extent to which starch granule characteristics vary in tomato fruit in different physiological, metabolic, and genetic backgrounds. This could broaden our understanding of starch biosynthesis in tomato and its control by changes in the internal environment of the fruit. There is good evidence that substrate concentration and organ physiology can influence the morphology, composition, and crystalline structure of starch from tuber, endosperm, and leaf (*6*−*10*). It is not known if tomato fruit starch would be similarly influenced. First, fruit of distinct sizes were compared, as this can influence sink capacity and potential for sugar import (*11*, *12*). Second, we looked at the effect of substrate supply on tomato granule characteristics by increasing the leaf-to-fruit ratio in two genotypes: Moneymaker and a high Brix-line Solara via pruning (*13*). Third, we asked if delayed ripening would affect starch granule structure. Two near-isogenic ripening mutants, *rin* (ripening-inhibitor) and *nor* (nonripening), and the normal parent line Ailsa Craig (*14*) were studied. Reduced climacteric ripening in the mutant may delay or reduce starch breakdown, thereby increasing starch levels. In addition, the mutants stay green longer and more starch may accumulate from fruit CO_2 fixation which accounts for up to 15% of starch synthesized (*15*). For all samples,

Published on Web 12/28/2009

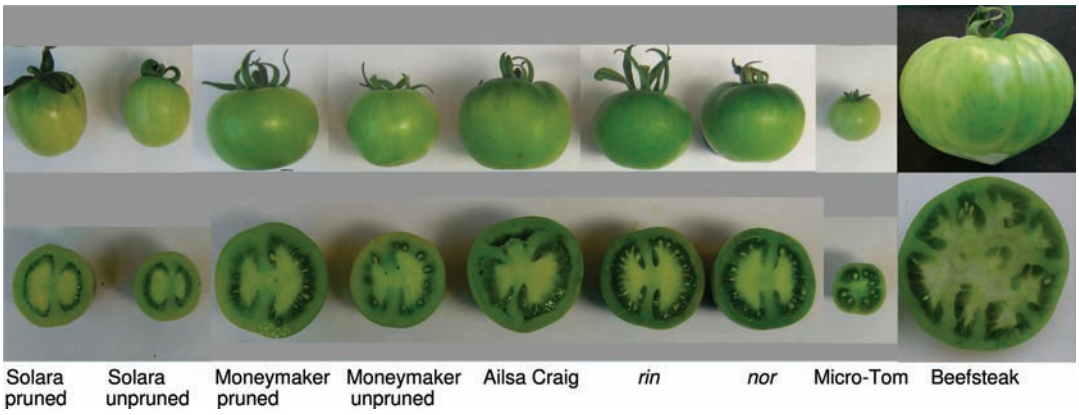

Figure 1. Mature green tomato fruit (40 DPA) of Beefsteak, Micro-Tom, Ailsa Craig, *rin*, *nor*, Moneymaker , and Solara with and without pruning. Solara and Moneymaker where the inflorescences were pruned are twice as large as those without pruning. Physical characteristics of Ailsa Craig, *rin*, and *nor* were essentially the same.

starch metabolism was assessed by measuring the amount accumulated at sampling, as well as the proportion synthesized from ^{14}C-glucose fed to fruit disks. Starch granule size, morphology, amylose-to-amylopectin ratio, crystallinity, glucan chain distribution, thermal properties, and rate of degradation by α-amylase were analyzed to develop a comprehensive picture of starch physiochemical structure. This study should expand our basic knowledge of starch characteristics in tomato.

MATERIALS AND METHODS

Reagents and Plant Materials. All chemicals were purchased from Sigma-Aldrich (St. Louis, MO) unless otherwise stated. Seeds of *Solanum lycopersicum* L. cv. Moneymaker, Ailsa Craig, *rin*, and *nor* were from the C. M. Rick Tomato Genetics Resource Center (TGRC; Davis, CA). Seeds of *Solanum pimpinellifolium* L. cv. Solara were a kind gift from Dr. Lilliana Stamova (Davis, CA). Seeds of Micro-Tom were a kind gift from Dr. David Weiss (The Hebrew University of Jerusalem, Israel). The Beefsteak variety was a gift from Seminis Vegetable Seeds (Woodland, CA).

Plant Growth Conditions and Fruit Sampling. Tomato plants were grown as described by Luengwilai and Beckles (*2*). Fruit developmental stage was recorded by tagging flowers after pollination on six individual plants for each genotype. For the pruning experiment, all but two flowers were removed from each inflorescence. All fruit used was harvested at mature green (MG), according to USDA standards (approximately 40 days post-anthesis (DPA)) (*1*). Whole fruit was weighed, and then 200−300 mg of fresh tissue was taken from the pericarp of each fruit for starch measurements. The rest of that fruit was used to determine dry weight by measuring the mass after 14 days in a ventilated oven at 55 °C.

Starch, Sugar, and Titratable Acidity Measurements. Starch extraction from the pericarp was as described by Luengwilai and Beckles (*2*). Glucose released from starch was assayed using the hexokinase glucose assay reagent (Sigma-Aldrich, St. Louis MO) as previously reported by Beckles et al. (*16*). Total soluble solids and titratable acidity (TA) was done as described by Luengwilai et al. (*17*).

Starch Granule Purification and Analysis. Starch granules were subjected to scanning electron and light microscopy, measurement of amylose content, particle size distribution, X-ray powder diffraction, and high performance size exclusion chromatography (HPSEC) after debranching starch. These analyses were done exactly as described by Luengwilai and Beckles (*2*).

α-Amylase Digestibility. Aliquots of 5 mg of starch were digested with α-amylase isolated from *Aspergillus niger* at a final concentration of 50 U/mg starch. The digestion volume was 0.5 mL, and the reaction was done in 200 mM sodium acetate buffer pH 4.8 at 37 °C for 0, 12, 24, 36, 48, and 60 h. The samples were spun at 15 000*g* for 10 min, and the pellet was washed three times in 80% (v/v) ethanol, five times with water, and then twice in 100% (v/v) acetone. The powder was allowed to dry by evaporation of acetone. The loss in weight of undigested starch was used to calculate the degree of hydrolysis. The supernatant was saved for measurements of glucose using a hexokinase kit as described previously. Three biological replicates, each consisting of starch extracted from different fruit, were used. Percentage of hydrolysis was calculated as follows:

$$\text{degree of hydrolysis (\% wet weight basis)} = \text{amount of glucose released (mg/mL)} \times \frac{162}{180} \times \frac{100}{\text{starch weight (mg)}}$$

Differential Scanning Calorimetry (DSC). Thermal properties of starch were measured using a Perkin−Elmer Diamond differential scanning calorimeter (Perkin-Elmer Co., Norwalk, CT) with Pyris operation software. The calorimeter was equipped with an Intracooler 2P apparatus (Perkin-Elmer) and nitrogen gas purge. An empty volatile sample pan was used as a reference. A starch-to-water ratio of 1:3 using ∼15 mg of starch was weighed into a volatile sample pan, hermetically sealed, and equilibrated overnight at room temperature prior to analysis. The sample and reference pans were scanned from 30 to 85 °C at a heating rate of 10 °C/min. Gelatinization temperatures were reported as onset temperature (T_o), peak temperature (T_p), and conclusion temperature (T_c). The range of gelatinization temperature (ΔT_g) was calculated by the difference between T_o and T_c. Enthalpy of gelatinization (ΔH) was calculated from the area of the gelatinization peak from the DSC thermogram.

Radiolabeling of Starch with ^{14}C-Glucose. Labeling of fruit disks (at the MG stage) was performed using methods established for tomato (*18*). Three biological replicates, each consisting of a single fruit, were used. The length of the incubation period was 2 h.

Statistical and Multivariate Analysis. All statistical analyses including PCA and calculation of loading scores were conducted in SAS version 9.1.3 software (SAS Institute Inc., Cary, NC). Comparison of means was performed by analysis of variance (ANOVA) followed by Tukey's test at 95% degree of confidence ($P \leq 0.05$). Correlative analyses were performed using Pearson's correlation coefficient where $n = 9$ samples × 3 biological replicates = 27.

RESULTS

Tomato Fruit Morphology and Mass Weight. The cultivars studied were grouped by physiological characteristics; one group was based on differences in fruit size (most disparate between Beefsteak and Micro-Tom), another on time-to-ripening (Ailsa Craig, *rin*, and *nor*), and the third on substrate availability (Solara and Moneymaker with or without pruning). Mature Green (MG) fruit was chosen for starch extraction because the total yield of starch is greatest at this stage (*1*).

Beefsteak fruit (∼200 g) was several-fold greater in mass than all cultivars and 40-fold greater than Micro-Tom (∼5 g) (**Figure 1**, Supporting Information Table 1). Moneymaker and Solara from pruned plants were twice as large as those from the unpruned

Table 1. Accumulation, Synthesis, Granule Characteristics, and Molecular Composition of Tomato Fruit Pericarp Starch at MG (40 DPA)[a]

genotypes	starch content (mg·gDW^{-1})	total soluble solids (%)	average granule size (μm)	% of granule <10 μm	amylose content (%)	degree of crystallinity (%)	total uptake of ^{14}C-glucose (Bq mgDW^{-1})	% of total ^{14}C-incorporated into starch
Beefsteak	52 ± 19 b	4.1 ± 0.1 e	17.0 ± 2.1 a	19.2 ± 2.9 b	23 ± 2 ns[b]	26 ± 2 ns[b]	18.6 ± 3.0 a	6.1 ± 1.3 ns[b]
Micro-Tom	137 ± 57 ab	6.1 ± 0.1 bc	11.1 ± 0.8 b	42.0 ± 4.8 a	22 ± 2	31 ± 0	9.8 ± 0.6 b	5.9 ± 0.7
Ailsa Craig	391 ± 95 a	6.7 ± 0.1 b	16.0 ± 0.4 a	20.6 ± 1.5 b	23 ± 0	31 ± 3	10.3 ± 0.3 b	5.7 ± 0.7
rin	204 ± 43 ab	5.0 ± 0.3 d	14.7 ± 0.3 a	23.6 ± 0.7 b	22 ± 1	26 ± 1	7.7 ± 0.4 b	4.4 ± 1.8
nor	196 ± 38 ab	4.9 ± 0.2 de	17.0 ± 0.9 a	17.4 ± 1.6 b	23 ± 0	27 ± 2	9.3 ± 1.3 b	3.3 ± 1.2
Solara pruned	188 ± 52 ab	9.5 ± 0.3 a	17.7 ± 0.6 a	18.2 ± 0.9 b	21 ± 1	28 ± 1	10.6 ± 1.3 b	6.8 ± 0.8
Solara unpruned	46 ± 25 b	9.1 ± 0.1 a	16.2 ± 0.7 a	21.1 ± 1.9 b	21 ± 1	29 ± 2	12.1 ± 0.4 b	3.5 ± 0.2
Moneymaker pruned	173 ± 41 ab	5.9 ± 0.6 c	17.5 ± 0.5 a	17.0 ± 0.7 b	19 ± 1	30 ± 4	8.5 ± 0.3 b	5.2 ± 1.0
Moneymaker unpruned	104 ± 17 ab	5.4 ± 0.1 cd	15.8 ± 0.3 a	21.0 ± 0.5 b	19 ± 0	28 ± 2	7.3 ± 0.4 b	7.9 ± 0.3

[a] Values are mean ± standard error of three different biological replicates. Means with different letters within the same column show a statistically significant difference ($p < 0.05$) by Tukey's test ($n = 3$) while means with the same letter do not. [b] ns: Means do not differ significantly within the column ($p < 0.05$) by Tukey's test ($n = 3$).

plants, while Ailsa Craig, *rin*, and *nor* fruit were similar in size (**Figure 1**, Supporting Information Table 1). From a quality perspective, Solara had the highest total soluble solids (9.5%) and Beefsteak had the lowest (4.1%). Micro-Tom had the highest TA values, and Solara and Moneymaker had the lowest (data not shown).

Starch Accumulation and ^{14}C-Metabolism to Starch. Starch content varied from 5 to 39% of fruit dry weight across samples (**Table 1**). Ailsa Craig had the highest starch content (391 ± 95 mg·gDW^{-1}), whereas Beefsteak and unpruned Solara had the lowest (52 ± 19 and 46 ± 25 mg·gDW^{-1}, respectively; **Table 1**). Although pruning increased fruit size (Supporting Information Table 1), this did not appear to alter starch content, as there was no statistically significant difference in the amount of starch assayed in the pruned versus unpruned samples (**Table 1**). There was also no difference in starch content between the ripening mutants, that is, *rin* and *nor*, and the normal parental line Alisa Craig (**Table 1**).

The flux of sugars to starch was estimated by feeding [U−^{14}C]-glucose to fruit pericarp disks. The total ^{14}C imported into the disk and the percentage of this ^{14}C incorporated into starch was assayed (**Table 1**). Only Beefsteak differed, showing a higher uptake of ^{14}C-glucose. In addition, the proportion of glucose that partitioned to starch over 2 h was identical among all samples, implying similar rates of starch synthesis (**Table 1**). This contrasts with the marked differences in starch accumulation recorded among some genotypes (**Table 1**).

Starch Granule Size and Morphology. Starch granules from all samples were spherical or oval in shape with two size populations when viewed by scanning electron microscopy (Supporting Information Figure 1). Similar to our previous reports (*2*), average granule size was 10−20 μm, as determined by laser diffraction. There were no significant differences in granule size distribution among genotypes except Micro-Tom, which had the smallest average size (11.1 ± 0.8 μm) and the greatest proportion (42%) of granules smaller than 10 μm (**Figure 2** and **Table 1**). Beefsteak showed the broadest distribution profile with granules bigger than 100 μm (**Figure 2**).

Amylose Content and Degree of Crystallinity. Starch is composed of two α-1-4-linked homoglucans called amylose and amylopectin and forms semicrystalline particles with varying degrees of crystallinity. Amylopectin exclusively determines crystallinity, while amylose is found in the amorphous (noncrystalline) region of the granule (*19*).

Amylose content and degree of crystallinity were not different among genotypes (**Table 1**). Amylose content at the MG stage was 19−23% (w/w), just slightly higher than tomato at 16 and 28 DPA (*2*). The X-ray crystallography of these starches indicated a C-type pattern with both the B-type (a strong peak at $2\theta = 17.2°$) and A-type (the lack of a split peak at $2\theta = 22-24°$ and a peak at 14.6°) peaks (Supporting Information Figure 2). Consistent with our previous work, the degree of crystallinity was 26−31% (**Table 1**) and was within the range of other C-type starches (*20*).

Starch Glucan Chain-Length Distribution. The backbone of the amylopectin molecule is branched with regular periodicity by α-1,6 linkages creating chains of defined lengths. The frequency of occurrence of the different chains dictates amylopectin organization within granules (*21*). Chain length distribution of dispersed tomato starch solutions after enzymatic debranching was analyzed using HPSEC. The chromatogram of the hydrolyzed starches showed four main peaks of chain-length fractions, which were designated as AmpF1, AmpF2, AmpF3, and AmpF4. These fractions were defined with inflection points at elution volumes of 16, 19.2, and 21 mL (**Figure 3**). AmpF1 contained extra-long chains of debranched amylopectin and debranched amylose. AmpF2, AmpF3, and AmpF4 contained long, medium, and short chains of debranched amylopectin, respectively. Average molecular weights (and calculated degree of polymerization, DP) of AmpF2, AmpF3, and AmpF4 fractions were approximately 60 000−250 000 (DP 370−1500), 10 000−50,000 (DP 60−300), and 4600−26 000 (DP 30−160), respectively. There was no significant difference among the genotypes studied except Beefsteak and Moneymaker (both pruned and unpruned), which had the highest and lowest molecular mass of long-chain amylopectin (Amp F2), respectively (**Table 2**).

The relative mass of the different fractions were then examined to get a better description of the frequency of the different amylopectin chain lengths identified in **Figure 3** within the starch granule. The concentrations of the chains in each of the defined fractions (**Figure 3**), that is, the long, medium, and short chains of amylopectin, are expressed as ratios relative to the long chain for easier comparisons (**Table 2**). Micro-Tom, Beefsteak, and Solara (both pruned and unpruned) exhibited a greater modal frequency of shorter chains (short/medium/long chain ratio = 7:3:1, 5:2:1, 4:1:1, and 4:2:1, respectively). In contrast, Ailsa Craig, *rin*, *nor*, and Moneymaker (both pruned and unpruned) had similar distributions of short/medium/long chains (2:1:1, 1:1:1, 2:1:1, and 1:1:1, respectively) (**Table 2**).

Differential Scanning Calorimetry. DSC gelatinization parameters can provide insight into starch granule structure. Gelatinization temperatures and differences in gelatinization enthalpy can be influenced by the degree of crystallinity and the length of the amylopectin chain involved in the crystalline unit as well as the proportion of double helical material (*22*, *23*). To our knowledge, there is no information on the thermal properties of tomato starch.

In excess water, tomato starch exhibited a single endothermic transition, having T_o values of 56.2−60.5 °C, T_p values of

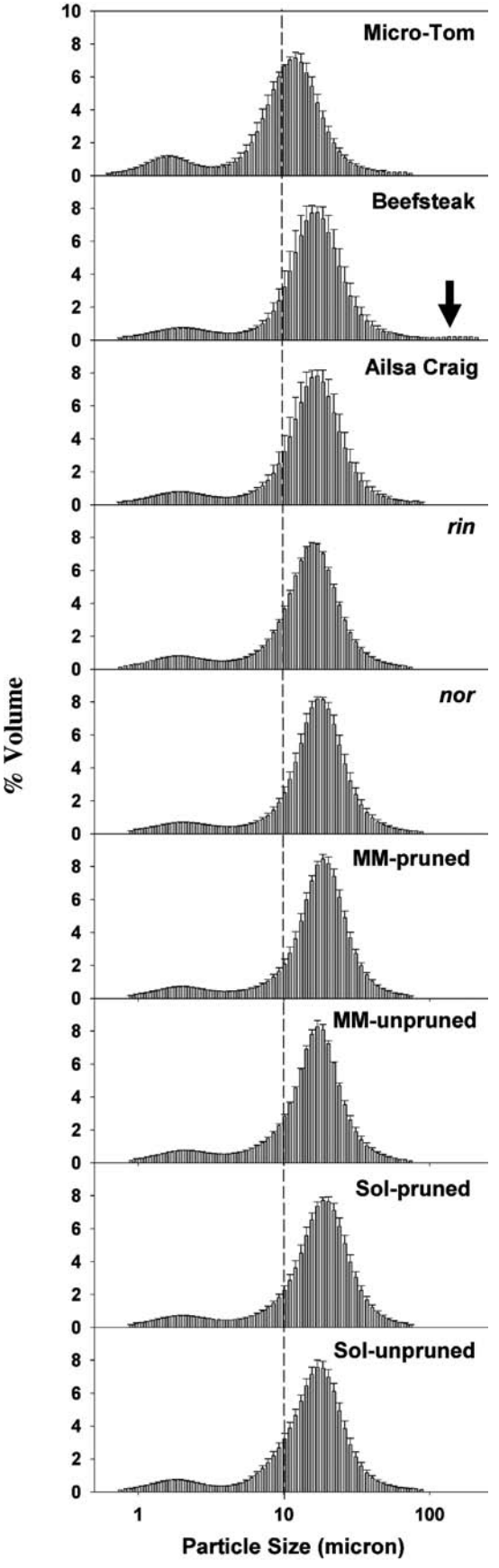

Figure 2. Particle size distribution of starch by laser diffraction. Each graph depicts the mean ± standard error of three biological replicates. Dashed lines indicate granules of 10 μm. Arrow indicate granules of >100 μm. Key: MM, Moneymaker; Sol, Solara.

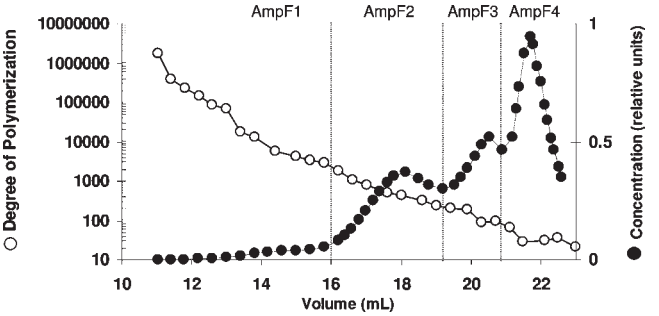

Figure 3. Molecular weight of four subfractions of debranched starch from Beefsteak by HPSEC-MALLS-RI. Fraction 1 (AmpF1) is predominantly amylose, while fractions 2, 3, and 4 (Amp F2, 3, and 4) are long, medium, and short chains of amylopectin, respectively. The degree of polymerization (DP) was calculated by dividing glucan M_w by 162 (mass of anhydrous glucose). Chromatographs were drawn for all samples and were used to calculate the data shown in **Table 2**.

61.2−67.2 °C, and T_c values of 68.5−75.0 °C (**Table 3**), which are within the range of normal starch (*7*). Micro-Tom possessed the highest T_o and T_p values, while these parameters were lowest for Moneymaker. All samples showed similar values of ΔT_g (11.7−13.8 °C), except Beefsteak, which manifested significantly higher values (16.8 °C). There was no significant difference in ΔH among the starches (**Table 3**).

Starch Enzymatic Hydrolysis. Tomato starches were incubated with α-amylase, and the kinetics of digestion was compared. Starch surface features, morphology, and internal structure (amylose/amylopectin ratio and their organization) may influence the rate of hydrolysis (*20*, *24*). Studies of starch from a range of species show that granule hydrolysis is initially rapid but then slows as the remnants become more resistant to the action of the hydrolytic agent (*25*). It is plausible that unique patterns of kinetics of *in vitro* starch hydrolysis may highlight important differences in starch structure. From a biological perspective, differences in starch structure could affect its degradation and could control the production of sugars during fruit ripening.

There were no differences in the initial hydrolysis of the nine tomato starch samples after 24 h (**Figure 4**). However, after 60 h, the Beefsteak and Micro-Tom starches were less susceptible to hydrolysis whereas unpruned Moneymaker and Solara were most sensitive. Consistent with their role in metabolism, tomato leaf (transitory) starch was digested more rapidly and potato tuber (storage) starch more slowly than tomato fruit starches (**Figure 4**).

Correlative Analysis and PCA. Pairwise correlations between the different parameters studied were established to identify potentially novel relationships between tomato starch parameters. Two parameters were considered to be correlated if $r \geq 0.45$ ($P < 0.01$). To check that *r*-values were not skewed by outliers (*26*), we plotted the data and recalculated the *r*-values after removing these distant points; those falling below 0.45 were excluded (Supporting Information Table 2).

Many of the starch structure parameters did not show strong correlations, and those that did were related to gelatinization temperatures. T_p, T_c, and ΔT_g correlated negatively with starch hydrolysis patterns (after 60 h), but T_o, T_p, and T_c varied positively with the fraction of smaller starch granules (< 10 μm) in the samples. ^{14}C-glucose uptake was positively related with fruit fresh weight and Brix positively correlated with the starch hydrolysis.

Principal component analysis (PCA) can provide an overview of the relatedness of the different starches based on the multiple parameters measured. Samples that group closely on the principal

Table 2. Molecular Weight (M_w), DP, and Mass Ratio of Three Subfractions of Debranched Starch from Tomato Starch by HPSEC-MALLS-RI[a]

	average M_w (g·mol^{-1})			average DP			mass ratio
genotypes	Amp F2	Amp F3	Amp F4	Amp F2	Amp F3	Amp F4	AmpF4:F3:F2
Ailsa Craig	138 797 ab	51 090 ns	15 929 ns	857	315	98	2:1:1
rin	107 980 ab	50 653	26 325	667	313	162	1:1:1
nor	205 467 ab	56 087	17 173	1268	346	106	2:1:1
Micro-Tom	123 643 ab	22 003	8695	763	136	54	7:3:1
Beefsteak	253 033 a	48 770	9581	1562	301	59	5:2:1
Moneymaker pruned	61 580 b	10 261	4590	380	63	28	1:1:1
Moneymaker unpruned	59 720 b	10 127	5736	369	63	35	1:1:1
Solara pruned	87 005 ab	28 890	10 013	537	178	62	4:1:1
Solara unpruned	92 037 ab	21 580	7611	568	133	47	4:2:1

[a] Fractions 2, 3, and 4 (Amp F2, 3 and 4) are long, medium, and short chains of amylopectin respectively. M_w is the molecular weight of the glucans and indicates the size of the chains based on molarity. Average DP indicates glucan chain length. The mass ratio is calculated from the concentration of glucans within each of the fractions defined in **Figure 3**. The proportions shown represent the concentration of long, medium, and small amylopectin chains expressed relative to the concentration of long chains.Values are mean ± standard error of three different biological replicates. Means with different letters within the same column differ significantly ($p < 0.05$) by Tukey's test ($n = 3$). ns: Means within the same column do not differ significantly ($p < 0.05$) by Tukey's test ($n = 3$).

Table 3. Gelatinization Properties of Various Tomato Starch Measured by DSC[a]

genotypes	T_o (°C)	T_p (°C)	T_c (°C)	ΔT_g (°C)	ΔH (J/g starch DW)
Beefsteak	58.2 ± 0.1 bc	66.8 ± 0.1 a	75.0 ± 0.2 a	16.8 a	16.5 ± 0.1 ns
Micro-Tom	60.5 ± 0.4 a	67.2 ± 0.3 a	74.4 ± 0.5 a	13.8 ab	15.0 ± 0.3
Ailsa Craig	58.8 ± 0.2 b	64.4 ± 0.1 b	71.3 ± 0.4 b	12.5 b	15.2 ± 0.4
rin	58.3 ± 0.0 bc	64.4 ± 0.0 b	71.9 ± 0.2 b	13.7 ab	14.9 ± 0.5
nor	57.1 ± 0.2 bcd	63.4 ± 0.3 bc	70.6 ± 0.3 bc	13.4 ab	14.8 ± 0.5
Solara unpruned	58.5 ± 0.2 bc	62.7 ± 0.3 bc	70.0 ± 0.8 bc	11.6 b	16.7 ± 0.2
Solara pruned	57.9 ± 0.4 bc	62.8 ± 0.2 bc	70.1 ± 0.8 bc	12.2 b	17.2 ± 0.3
Moneymaker unpruned	56.8 ± 1.4 cd	61.4 ± 1.8 c	68.5 ± 1.8 c	11.7 b	15.7 ± 1.3
Moneymaker pruned	56.2 ± 0.4 d	61.2 ± 0.2 c	68.5 ± 0.5 c	12.2 b	15.3 ± 0.4

[a] T_o = onset temperature, T_p = peak temperature, T_c = conclusion temperature, ΔH = enthalpy (J/g starch), ΔT_g = gelatinization range ($T_c - T_o$) (°C). Values are mean ± standard error of three different biological replicates. Means with different letters within the same column differ significantly ($p < 0.05$) by Tukey's test ($n = 3$). ns: Means within the same column do not differ significantly ($p < 0.05$) by Tukey's test ($n = 3$).

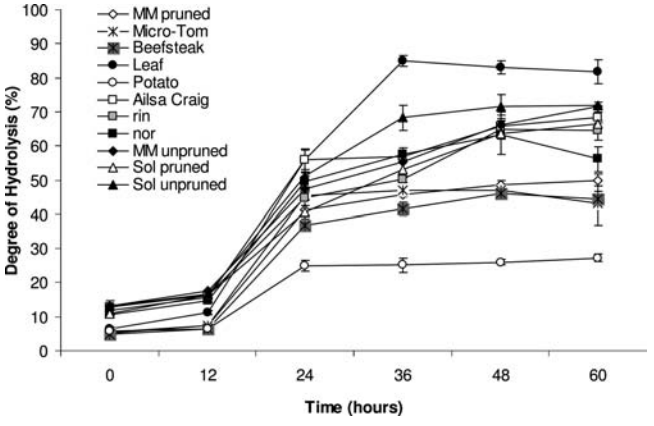

Figure 4. Pattern of hydrolysis of tomato starch after digestion by α-amylase. Potato and tomato leaf starch were included as references of storage and transitory starch, respectively. Values are mean ± SE of three different biological replicates. Key: MM, Moneymaker; Sol, Solara.

component (PC) are more similar to each other, while less similar samples are on distant coordinates. Three groups can be discerned on the PCA plot. Ailsa Craig, *rin* and *nor*, Solara and Moneymaker with or without pruning grouped together, whereas Beefsteak and especially Micro-Tom were outliers (**Figure 5A**). By examining the loading scores of the PC, the relative importance or absolute magnitude of each variable within each PC can be discerned. Variables that cluster around the origin have little effect on the PC, whereas those that are further apart make a greater contribution. $\mathbf{T}_p$, percent of granule size < 10 μm (small granule), and average granule size (psa) explained the separation seen in PC1 (29%), while the relative mass ratio of long- and short-length chains (AmpF2, AmpF4) and enthalpy (ΔH) explained the separation seen in PC2 which accounted for 21% of the variability (**Figure 5B**). The fact that the PCs only explained 29 and 21% of the variation between samples highlights that starch properties of all samples were very similar.

DISCUSSION

Our aim was to examine starch biosynthesis in different tomato samples and determine if this has an effect on starch structure. This could inform generally on the nature of starch biosynthesis and provide more insight on "transitory-storage" starches. The results presented here indicate that starch granule structure in tomato fruit is fairly constant across genotypes and that few features are responsive to changes in cellular conditions. Granules from fruit differing in size, ripening behavior, and substrate availability (by pruning) did not show any consistent pattern related to their phenotype or even their genotype. This is remarkable given that we demonstrated the extent to which these fruit differed in starch metabolism: the percentage of starch accumulated varied 10-fold among some samples, and therefore, metabolism may vary widely over the 40 days prior to sampling which might be reflected in structure. However, in spite of these differences, granule characteristics were similar (**Table 1**).

Starch synthesis alone may not determine starch accumulation in tomato fruit. The capacity for synthesis was similar in all samples we examined, but the amount of starch accumulated, as mentioned earlier, varied 10-fold. A noteworthy example is the Beefsteak tomato. This cultivar imported 1.5−2.5-fold more labeled glucose than the others compared and should have a

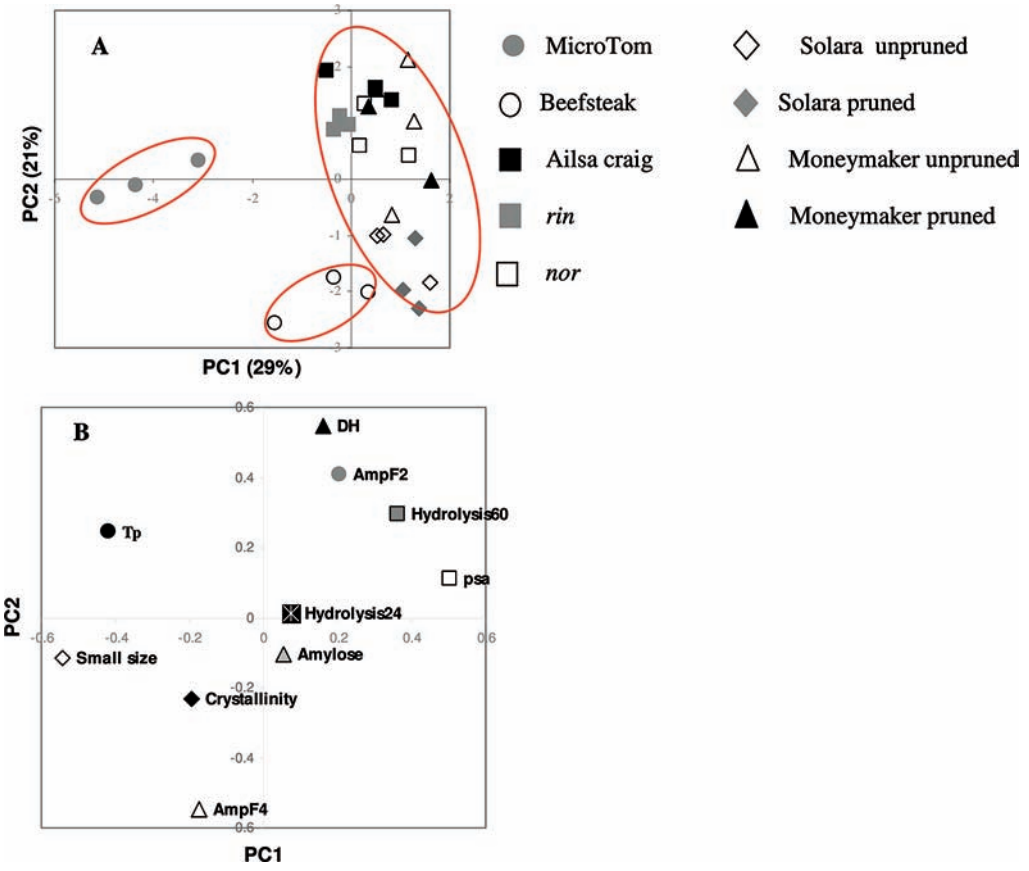

Figure 5. (**A**) PCA of all structural variables of tomato samples studied. The first two principal components were plotted. Tomato fruit with similar starch characteristics will cluster together, while outliers will form separate groups. (**B**) PCA loading scores and percent variance that explained each of the components presented in (**A**). Loading scores specify the magnitude of each variable in contributing the principal components. Key: psa, average granule size; small size, percentage of granules < 10 μm; AmpF2 and AmpF4, molecular weights of amylopectin fraction 2 and 4, respectively, after isoamylase hydrolysis; T_p, peak temperature; ΔH, enthalpy (J/g starch); Hydrolysis24 and Hydrolysis60, glucose released after α-amylase starch hydrolysis for 24 and 60 h incubation, respectively.

similar or greater amount of starch synthesized, since the percentage of this label that partitioned to starch was identical to that in the other tomatoes (**Table 1**). However, Beefsteak accumulated 2−4-fold *less* starch than other samples. The discrepancy between the amount of starch synthesized and the amount accumulated can be explained if the starch is being degraded (**Table 1**). We have previously shown that there is simultaneously synthesis and degradation of starch in Moneymaker fruit (*1*), and turnover may also occur in other tomato cultivars (*5*). Pulse-chase experiments would be needed to prove definitively that the starches in the cultivars examined are also subjected to turnover. Still, overall, the data in this study points to this possibility that starch accumulation is regulated differently among genotypes.

Our data are consistent with the idea that increased sink strength in larger fruit is determined by increases in cell division and less so by cell volume. Our work showed that sink strength, that is, the ability to take up sugars, was greatest in the large-fruited Beefsteak cultivar (**Table 1**). This was not seen when fruit size increased from pruning. Varying rates of cell division are generally regarded as the basis for differences in fruit size between most tomato genotypes, while an increase in cell volume usually explains increased fruit size from pruning (*27*). Therefore, larger cell volume may be less important in determining sink capacity than the number of cells.

It is known that very long or very short chains (within certain optimal limits) and their molar masses can increase the stability of crystalline lamellae in a starch granule (*22*), and we wanted to identify parameters that would have such an effect in tomato. Both Beefsteak and Micro-Tom had a high proportion of short chains (7:3:1 and 5:2:1) of DP (54−59) and these starches had highest gelatinization temperature, implying enhanced stability of crystallites within a granule (**Tables 2** and **3**). Therefore, chains with these characteristics could promote double helical formation within the crystalline lamellae increasing their rigidity. However, Solara also had a high proportion of short chains (4:2:1) of DP 55, quite similar to the case of Micro-Tom, but its gelatinization temperatures were lower. The only other difference was the DP of the long chains (Amp 2), which was ~550 in Solara, significantly lower than that in Beefsteak (1562) and Micro-Tom (763) (**Tables 2** and **3**). Thus, there may also be a role for long chains in reinforcing granule stability even if they occur at low frequency. We also noticed that Moneymaker starch had the smallest DP for each chain length fraction and they may have led to the low gelatinization temperatures for this sample (**Tables 2** and **3**).

Few generalizations can be made about structure−property relationships of tomato starches from this study. Some observations however make sense in the context of what is known about starch, while others may be novel. We established that

(i) Unlike other starches (*7*, *22*), differences in gelatinization temperature were not caused by differences in the degree of crystallinity, as these were similar across samples (**Tables 1** and **3**).

(ii) A complex set of factors determines susceptibility of starch to hydrolysis. Pruning (in both Moneymaker and Solara) increased the resistance of starch to enzymatic hydrolysis. This may be through some

unknown mechanism because there were no other differences in starch metabolism between these samples.We also found that starches with the highest gelatinization temperatures (Beefsteak and Micro-Tom) also showed high recalcitrance to enzymatic hydrolysis after 60 h, indicating greater stability of the crystallites (**Table 3**, **Figure 4**). For the Beefsteak sample, the high M_w of the long chain fraction might also have contributed to this resilience (*28*, *29*). The results of the enzyme digestibility experiment would appear to contradict our conclusion that Beefsteak starch is subject to greater rates of starch degradation during synthesis than in the other genotypes. There is however no overlap between the two experiments. The ^{14}C-glucose feeding experiment was done using an *in vivo* system, whereas the enzyme digestibility was performed using highly artificial *in vitro* conditions. In this experiment, purified starch isolated from the cellular environment was used, as were high, nonphysiological amounts of α-amylase activity. This *in vitro* data therefore cannot be used to draw conclusions on starch metabolism but is important for identifying structural differences between starches.

(iii) The affect of granule size on tomato starch characteristics may not be significant. There was no relationship between granule size and any other starch structure measurement. The granule surface area-to-volume ratio influences granule structure−function in other species (*10*, *29*, *30*), but Micro-Tom and Beefsteak, which had the smallest and largest granule size distributions, had similar gelatinization temperatures, starch hydrolysis patterns, and glucan chain-length distribution (**Figures 2** and **4**). However, a possible relationship between granule size distribution and gelatinization behavior was found. Beefsteak starch, which showed the broadest granule size distribution, also had the greatest gelatinization temperature range (ΔT_g) (**Figure 2** and **Table 3**). This could imply that Beefsteak contained a mixture of small-to-large starch granules with different thermal stabilities.

(iv) A positive relationship was found between Brix and starch hydrolysis in this study. This finding supports the view that in some cultivars starch can contribute to ripe fruit soluble solids (*4*).

Our research extends knowledge of factors influencing starch granule characteristics in plants. We showed that starch accumulation in tomato fruit is appreciable up to 39% (w/w) in some cultivars. However, most of the tomato starches had similar structure and properties in spite of differences in starch accumulation and metabolism. The highly conserved nature of the starch granule three-dimensional architecture found in different genetic, physiological, and biochemical backgrounds presented here suggests that there are intrinsic mechanisms that limit variations in starch structure in tomato fruit.

ACKNOWLEDGMENT

We thank Glorietta Hurd and Pamela Chacha for technical assistance.

Supporting Information Available: Supplemental Table 1: Fruit fresh weight and the dry weight to fresh weight ratio of different tomato cultivars. Fresh weight was measured from pericarp at MG stage and dry weight was measured from the same tissue after 14 days in a ventilated oven at 55 °C. Values are mean ± SE of six different biological replicates. Supplemental Table 2: Pearson correlation coefficients for all measured properties of starches of different tomato cultivars. All fruit physiological and physicochemical properties of nine different tomato starch samples (n = 9 samples × 3 replicates = 27) were used. Note that minor correlated parameters are not shown. Data were significantly different at $P < 0.01$. Supplemental Figure 1: Scanning electron micrographs of purified starch granules from MG tomato fruit. Magnification = 500×. The bar scale is 50 μm. Supplemental Figure 2: Representative X-ray powder diffractogram of starch purified from different cultivars at MG using a Scintag X-ray diffractometer. Crystallinity was calculated on three different biological replicates for each sample. Arrows indicate a peak at 14.6°, a strong peak at 2θ = 17.2°, and the lack of a split peak at 2θ = 22−24°. This material is available free of charge via the Internet at http://pubs.acs.org.

LITERATURE CITED

(1) Luengwilai, K.; Beckles, D. M. Starch Granules in Tomato Fruit Show a Complex Pattern of Degradation. *J. Agric. Food Chem.* **2009**, *57* (18), 8480–8487.

(2) Luengwilai, K.; Beckles, D. M. Structural Investigations and Morphology of Tomato Fruit Starch. *J. Agric. Food Chem.* **2009**, *57* (1), 282–291.

(3) Petreikov, M.; Yeselson, L.; Shen, S.; Levin, I.; Schaffer, A. A.; Efrati, A.; Bar, M. Carbohydrate Balance and Accumulation during Development of Near-isogenic Tomato Lines Differing in the AGPase-L1 Allele. *J. Am. Soc. Hortic. Sci.* **2009**, *134* (1), 134–140.

(4) Dinar, M.; Stevens, M. A. The Relationship between Starch Accumulation and Soluble Solids Content of Tomato Fruits. *J. Am. Soc. Hortic. Sci.* **1981**, *106* (4), 415–418.

(5) N′tchobo, H.; Dali, N.; Nguyen-Quoc, B.; Foyer, C. H.; Yelle, S. Starch synthesis in tomato remains constant throughout fruit development and is dependent on sucrose supply and sucrose synthase activity. *J. Exp. Bot.* **1999**, *50* (338), 1457–1463.

(6) Pilling, E.; Smith, A. M. Growth ring formation in the starch granules of potato tubers. *Plant Physiol.* **2003**, *132* (1), 365–371.

(7) Singh, N.; Singh, J.; Kaur, L.; Sodhi, N. S.; Gill, B. S. Morphological, thermal and rheological properties of starches from different botanical sources. *Food Chem.* **2003**, *81* (2), 219–231.

(8) Wootton, M.; Mahdar, D. Properties of Starches from Australian Wheats 0.3. In-Vitro Digestibility and Hydroxypropyl Derivatives. *Starch/Staerke* **1993**, *45* (10), 337–341.

(9) Xu, L. J.; Xie, J. K.; Kong, X. L.; Bao, J. S. Analysis of genotypic and environmental effects on rice starch. 2. Thermal and retrogradation properties. *J. Agric. Food Chem.* **2004**, *52* (19), 6017–6022.

(10) Zeeman, S. C.; Tiessen, A.; Pilling, E.; Kato, K. L.; Donald, A. M.; Smith, A. M. Starch synthesis in arabidopsis. Granule synthesis, composition, and structure. *Plant Physiol.* **2002**, *129* (2), 516–529.

(11) Bertin, N.; Causse, M.; Brunel, B.; Tricon, D.; Genard, M. Identification of growth processes involved in QTLs for tomato fruit size and composition. *J. Exp. Bot.* **2009**, *60* (1), 237–248.

(12) Walker, A. J.; Ho, L. C.; Baker, D. A. Carbon Translocation in Tomato - Pathways of Carbon Metabolism in Fruit. *Ann. Bot.* **1978**, *42* (180), 901–909.

(13) Prudent, M.; Causse, M.; Genard, M.; Tripodi, P.; Grandillo, S.; Bertin, N. Genetic and physiological analysis of tomato fruit weight and composition: influence of carbon availability on QTL detection. *J. Exp. Bot.* **2009**, *60* (3), 923–937.

(14) Giovannoni, J. J. Fruit ripening mutants yield insights into ripening control. *Curr. Opin. Plant Biol.* **2007**, *10* (3), 283–289.

(15) Obiadalla-Ali, H.; Fernie, A. R.; Lytovchenko, A.; Kossmann, J.; Lloyd, J. R. Inhibition of chloroplastic fructose 1,6-bisphosphatase in tomato fruits leads to decreased fruit size, but only small changes in carbohydrate metabolism. *Planta* **2004**, *219* (3), 533–540.

(16) Beckles, D. M.; Craig, J.; Smith, A. M. ADP-glucose pyrophosphorylase is located in the plastid in developing tomato fruit. *Plant Physiol.* **2001**, *126* (1), 261–266.

(17) Luengwilai, K.; Sukjamsai, K.; Kader, A. A. Responses of ′Clemenules Clementine′ and ′W. Murcott′ mandarins to low oxygen atmospheres. *Postharvest Biol. Technol.* **2007**, *44* (1), 48–54.
(18) Carrari, F.; Baxter, C.; Usadel, B.; Urbanczyk-Wochniak, E.; Zanor, M. I.; Nunes-Nesi, A.; Nikiforova, V.; Centero, D.; Ratzka, A.; Pauly, M.; Sweetlove, L. J.; Fernie, A. R. Integrated analysis of metabolite and transcript levels reveals the metabolic shifts that underlie tomato fruit development and highlight regulatory aspects of metabolic network behavior. *Plant Physiol.* **2006**, *142* (4), 1380–1396.
(19) Zobel, H. F. Molecules to Granules - a Comprehensive Starch Review. *Starch/Staerke* **1988**, *40* (2), 44–50.
(20) Stevenson, D. G.; Doorenbos, R. K.; Jane, J. L.; Inglett, G. E. Structures and functional properties of starch from seeds of three soybean (Glycine max (L.) Merr.) varieties. *Starch/Staerke* **2006**, *58* (10), 509–519.
(21) Hizukuri, S. Polymodal Distribution of the Chain Lengths of Amylopectins, and Its Significance. *Carbohydr. Res.* **1986**, *147* (2), 342–347.
(22) Parker, R.; Ring, S. G. Aspects of the Physical Chemistry of Starch. *J. Cereal Sci.* **2001**, *34* (1), 1–17.
(23) Vandeputte, G. E.; Delcour, J. A. From sucrose to starch granule to starch physical behaviour: a focus on rice starch. *Carbohydr. Polym.* **2004**, *58* (3), 245–266.
(24) Valetudie, J. C.; Colonna, P.; Bouchet, B.; Gallant, D. J. Hydrolysis of Tropical Tuber Starches by Bacterial and Pancreatic Alpha-Amylases. *Starch/Staerke* **1993**, *45* (8), 270–276.
(25) Oates, C. G. Towards an understanding of starch granule structure and hydrolysis. *Trends Food Sci. Technol.* **1997**, *8* (11), 375–382.
(26) Stamova, B. S.; Roessner, U.; Suren, S.; Laudencia-Chingcuanco, D.; Bacic, A.; Beckles, D. M. Metabolic profiling of transgenic wheat over-expressing the high-molecular-weight Dx5 glutenin subunit. *Metabolomics* **2009**, *5* (2), 239–252.
(27) Ho, L. C. The mechanism of assimilate partitioning and carbohydrate compartmentation in fruit in relation Ito the quality and yield of tomato. *J. Exp. Bot.* **1996**, *47*, 1239–1243.
(28) Salman, H.; Blazek, J.; Lopez-Rubio, A.; Gilbert, E. P.; Hanley, T.; Copeland, L. Structure-function relationships in A and B granules from wheat starches of similar amylose content. *Carbohydr. Polym.* **2009**, *75* (3), 420–427.
(29) Ao, Z. H.; Jane, J. L. Characterization and modeling of the A- and B-granule starches of wheat, triticale, and barley. *Carbohydr. Polym.* **2007**, *67* (1), 46–55.
(30) Roldan, I.; Wattebled, F.; Lucas, M. M.; Delvalle, D.; Planchot, V.; Jimenez, S.; Perez, R.; Ball, S.; D′Hulst, C.; Merida, A. The phenotype of soluble starch synthase IV defective mutants of Arabidopsis thaliana suggests a novel function of elongation enzymes in the control of starch granule formation. *Plant J.* **2007**, *49* (3), 492–504.

Received for review September 16, 2009. Revised manuscript received November 19, 2009. Accepted December 2, 2009. The Anandamahidol Foundation supported K.L. This work was funded by National Science Foundation Grant MCB-0620001, France Berkeley Fund Award, and Hatch Projects CA-D*-PLS-7198-H and CA-D*-PLS-7821-H to D.M.B.